

Frequency mixing of photorefractive and ferroelectric gratings in lithium niobate crystals

U. Hartwig, M. Kösters, Th. Woike, and K. Buse

Institute of Physics, University of Bonn, D-53115 Bonn, Germany

A. Shumelyuk and S. Odoulov

Institute of Physics, National Academy of Sciences, 252650 Kiev, Ukraine

Received October 25, 2005; revised November 21, 2005; accepted November 21, 2005; posted November 29, 2005 (Doc. ID 65584)

Holographically recorded photorefractive gratings in periodically poled lithium niobate crystals (PPLNs) are investigated. The principal spatial frequency K of the grating is strongly suppressed. Sideband gratings with grating vectors $\mathbf{K} \pm \mathbf{G}$ appear. From the measurements the domain grating vector \mathbf{G} and the duty cycle of the domain structure can be obtained. These findings allow for fast nondestructive quality inspection of PPLN and are of importance for any optical application combining holography and PPLN. © 2006 Optical Society of America

OCIS codes: 090.2900, 090.7330, 120.4630.

Periodically poled lithium niobate crystals (PPLNs) are of great importance for many applications in nonlinear optics such as second-harmonic generation (SHG) or optical parametric oscillation (OPO).¹ The interest in doped, photorefractive PPLN has grown recently due to the fact that it enables holographic recording but suppresses long-range index changes^{2,3} that are present in lithium niobate crystals without structured domains. Most of the doped PPLN samples studied so far were grown directly by using a periodic modulation of the growth condition.⁴ They generally have a less pronounced far order compared with that of PPLN fabricated with the help of structured electrodes. This is relevant since for frequency conversion the long-range order of the domain pattern is of importance to ensure that the phase-matching condition is valid throughout the crystal. Furthermore, the abilities of frequency conversion and holographic recording are simultaneously needed to realize a distributed feedback OPO.⁵

A detailed theory of holography in PPLN has been developed.⁶ It was predicted that the holographic grating mixes with the domain grating. Such an influence of the domain grating has been shown in holographic scattering experiments.⁷

In this work we show that, next to the principal grating \mathbf{K} , sideband gratings with grating vectors $\mathbf{K} \pm \mathbf{G}$, \mathbf{G} being the domain grating vector, appear in standard holographic experiments. The diffraction efficiency $\eta^{\pm 1}$ of the sideband gratings can exceed the diffraction efficiency η^0 of the principal grating. This is the first experimental proof, to our knowledge, that a photorefractive grating can be recorded in PPLN not only with bulk photovoltaic charge transport³ but also with diffusion-driven charge separation. Furthermore, we show that by measuring the normalized efficiency η_1/η_0 it is possible to deduce the duty cycle (DC) averaged over the cross section of the recording light beams.

The experiments are performed with copper-doped and therefore photorefractive PPLN. To prepare the samples, first a 150 nm copper layer is superimposed on the $-z$ side of a single-domain lithium niobate

crystal wafer. The layer is then indiffused by thermal treatment.⁸ The $-z$ side is chosen to prevent a surface domain pattern after indiffusion as described in Ref. 9. By utilizing structured electrodes and electrical fields, periodic domain inversion is obtained.¹⁰ The domain grating is orientated along the x axis of the wafer, its period length is $L=30 \mu\text{m}$, and hence the length of the grating vector is $G=0.21 \mu\text{m}^{-1}$. The dimensions of a sample are $x \times y \times z=16 \text{ mm} \times 15 \text{ mm} \times 0.5 \text{ mm}$. By this structuring process a well-defined long-range order of the domain structure is obtained.

The experiments are performed by using a two-beam interference setup. Two ordinarily polarized light beams of equal intensity, coming from an Ar⁺ laser operating at $\lambda_{\text{rec}}=488 \text{ nm}$, are incident symmetrically on the x, y face of the sample. The angle of the beams with respect to the normal of the surface plane inside the crystal is $\theta_{\text{rec}}=12.20^\circ$. So the length of grating vector \mathbf{K} can be calculated as follows: $\mathbf{K}=4\pi n_{o,\text{rec}}\lambda_{\text{rec}}^{-1} \sin \theta_{\text{rec}}=12.78 \mu\text{m}^{-1}$, where $n_{o,\text{rec}}$ is the refractive index for ordinarily polarized light at the recording wavelength.¹¹ The grating vector is parallel to the x axis of the crystal. In this geometry the only charge driving force is diffusion. The corresponding tensor element β_{122} for the bulk photovoltaic current is zero due to the crystal symmetry. This also holds true for electro-optic tensor elements r_{221} and r_{111} .¹² As a result, no isotropic diffraction is possible in this special geometry. However, anisotropic diffraction, which can be distinguished by a 90° change of the light polarization angle, is possible. The corresponding tensor elements r_{121} and r_{211} are nonzero. For readout an ordinarily polarized He-Ne laser beam with a wavelength of $\lambda_{\text{read}}=633 \text{ nm}$ is used. The angle inside the crystal θ_{read}^0 for the readout light can be calculated from the following equation:

$$K = \sin \theta_{\text{read}}^0 \left(\frac{2\pi n_{o,\text{read}}}{\lambda_{\text{read}}} + \frac{2\pi n_{e,\text{read}}}{\lambda_{\text{read}}} \right), \quad (1)$$

where $n_{o,\text{read}}$ and $n_{e,\text{read}}$ are the refractive indices for light polarized perpendicular and parallel to the z axis at the readout wavelength, respectively.¹¹ Figure

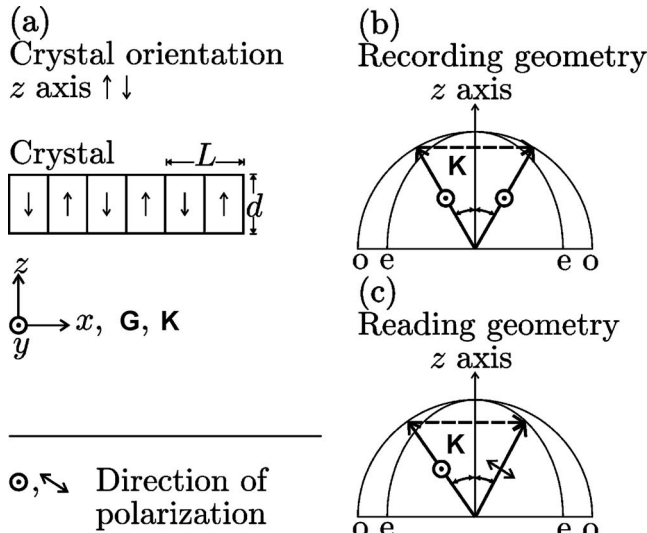


Fig. 1. Schematic illustration of the crystal orientation: (a) x axis and grating vectors \mathbf{G} and \mathbf{K} are parallel, (b) recording light is ordinarily polarized; (c) incident beam is polarized ordinarily, and the readout process is purely anisotropic.

1 summarizes the crystal orientation and the recording and readout geometries.

At the calculated angle of Bragg incidence $\theta_{\text{read}}^0 = 16.68^\circ$ for the principal grating a diffracted beam is observed. The corresponding selectivity curve is shown in Fig. 2(a). The maximum diffraction efficiency is $\eta_{\text{max}}^0 \approx 1 \times 10^{-4}$.

In addition to the diffracted light from the principal grating, more diffracted light is observed at different readout angles. In Figs. 2(b) and 2(c) the selectivity curves appearing next to the selectivity curve of the principal grating are presented. The maximum diffraction efficiencies $\eta_{\text{max}}^{\pm 1} \approx 5 \times 10^{-4}$ of the curves are almost equal. The angles of the observed maxima are $\theta_{\text{Bragg}}^{-1} = 16.39^\circ$ and $\theta_{\text{Bragg}}^{+1} = 16.95^\circ$. By plugging the measured angles of Bragg incidence into Eq. (1), the grating length of the vectors of these sideband gratings can be calculated ($K^{-1} = 12.57 \pm 0.01 \mu\text{m}^{-1}$ and $K^{+1} = 12.99 \pm 0.01 \mu\text{m}^{-1}$). Thus the diffracted light can be assigned to the sideband gratings with grating vectors $\mathbf{K}^{\pm 1} = \mathbf{K} \pm \mathbf{G}$.

The appearance of the sideband gratings can be understood by Fourier analysis of the grating structure. In our geometry charges are driven by diffusion alone, which is independent of the domain orientation. Therefore the electric space-charge field $E_1(x)$ has basically a sinusoidal shape throughout the crystal. The modulation of the permittivity tensor, $\delta\epsilon_{21}(x)$, however, is a sinusoidal pattern interrupted by periodic π phase shifts at the domain walls because of periodic domain inversion. As a result we can write for the component of the permittivity tensor change $\delta\epsilon_{21}(x) \approx -n^4 r_{211} E_1(x) p(x)$, where n is the average refractive index for ordinarily and extraordinarily polarized light. The function $p(x)$ is either +1 or -1, depending on the orientation of the spontaneous polarization of the domain because of the changing sign of the electro-optic coefficient.⁷

The Fourier analysis of such a pattern yields components of the original holographic \mathbf{K} grating and resulting sideband gratings $\mathbf{K} \pm \mathbf{sG}$, with \mathbf{s} being a natural number.⁶ From the Kogelnik equation¹³ it follows that $\eta \propto \delta\epsilon_{21}(x)^2$ for small diffraction efficiencies. From this we derive the following equation:

$$\frac{\eta^{\pm s}}{\eta^0} = \left[\frac{2 \sin(s\pi DC)}{s\pi(1 - 2DC)} \right]^2. \quad (2)$$

Here DC is defined as $DC = x_+ / (x_+ + x_-)$, where x_+ and x_- are the widths of domains with a spontaneous polarization pointing in the $+z$ and $-z$ directions, respectively. Thus $DC = 0.5$ is the optimum for quasi-phase matching. The transcendental Eq. (2) is plotted in Fig. 3. The dashed lines indicate the resulting DC for our experiment: A ratio of $\eta^{\pm 1}$ to η^0 equal to 5 gives us a value of the duty cycle of $DC = 0.37 \pm 0.005$. For an ideal PPLN structure, $DC = 0.5$, the central peak of the primary grating disappears. Experiments with less perfect PPLN samples yield smaller values of the duty cycle DC. After etching of the sample,¹⁴ which is studied in this work, an optical inspection of its surface yields an averaged value of $DC = 0.41 \pm 0.02$.

It is important to underline that the DC value extracted in this way is not affected by other possible contributions to the nonlinear grating. The diffraction from all imaginable other light-induced gratings,

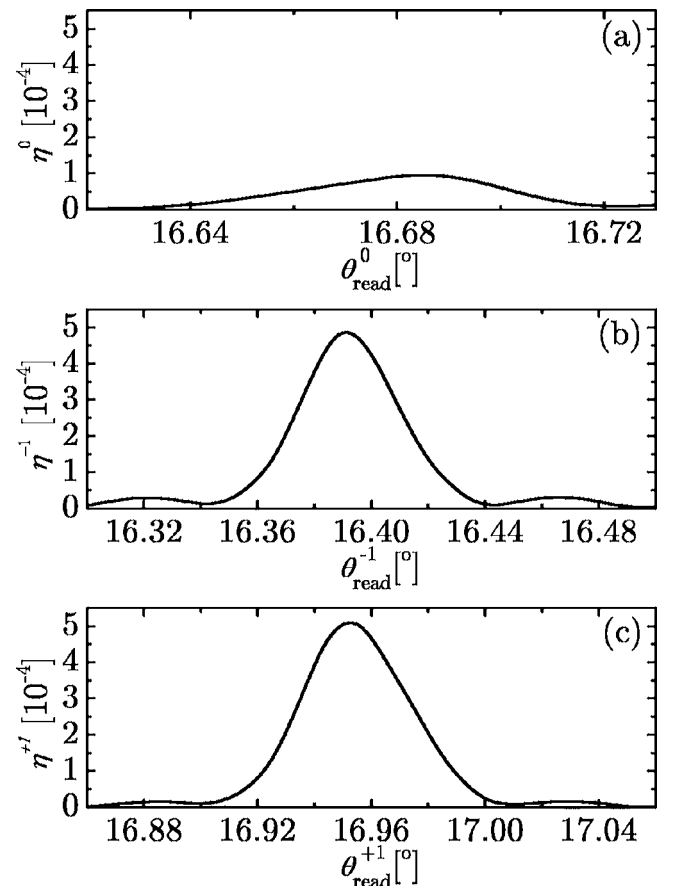


Fig. 2. Selectivity curves of (a) principal grating K , (b) sideband grating $\mathbf{K} - \mathbf{G}$, (c) sideband grating $\mathbf{K} + \mathbf{G}$.

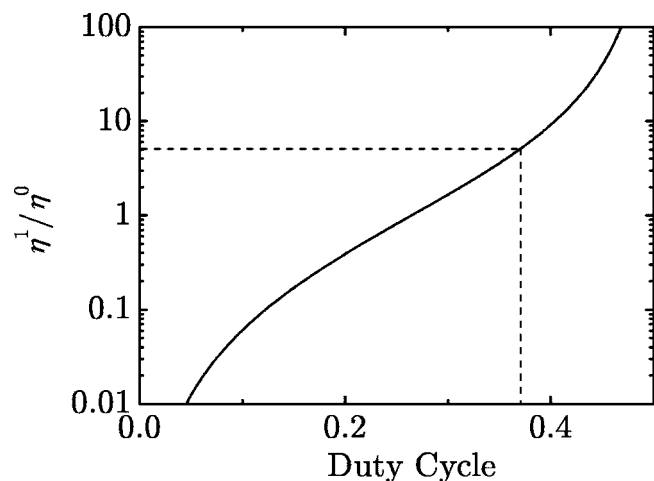


Fig. 3. Determination of the DC of the domain structure: solid curve, calculated from Eq. (2), dashed lines, measured ratio of η^1 to η^0 .

including gratings that are due to nonlinear absorption and Kramers–Kronig index variations,¹⁵ is isotropic and can easily be filtered out from the orthogonally polarized signal that defines the diffraction efficiency.

The proposed technique of PPLN inspection is complementary to those based on second-harmonic generation¹⁶ or on photorefractive beam coupling.^{17,18} As distinct from all these traditional methods that give 2D maps of domains with opposite orientation of the spontaneous polarization, our technique allows one to evaluate an averaged value of the duty cycle within the area covered by the recording light beams.

The introduced technique is extremely sensitive to deviations of the duty cycle DC from the optimum value 0.5 (see Fig. 3). Unlike etching techniques,¹⁴ this method is nondestructive. The holographic gratings can be erased easily by heating the crystal to 200°C. Undoped PPLN samples can in principle also be examined by holography using UV or pulsed laser light.^{19–21}

For any application that utilizes photorefractive gratings in PPLN, e.g., distributed feedback optical parametric oscillators,⁵ it has to be considered that the main peak is strongly suppressed. Thus, for such applications the photorefractive grating must be intentionally written with a spatial frequency larger or smaller by G than one would expect at first glance.

Financial support from the Deutsche Telekom AG, the Alexander von Humboldt Foundation (Research Award to S. Odoulov) and from the DFG (FOR 557) is gratefully acknowledged. U. Hartwig's e-mail address is hartwig@physik.uni-bonn.de.

References

1. L. Arizmendi, *Phys. Status Solidi A* **201**, 253 (2004).
2. A. Ashkin, A. C. D. Boyd, J. M. Dziedzic, R. G. Smith, A. A. Ballman, J. J. Levinstein, and K. Nassau, *Appl. Phys. Lett.* **9**, 72 (1966).
3. S. Odoulov, T. Tarabrova, A. Shumelyuk, I. I. Naumova, and T. O. Chaplina, *Phys. Rev. Lett.* **84**, 3294 (2000).
4. I. I. Naumova, N. F. Evalanova, O. A. Gilko, and S. V. Lavrishchev, *J. Cryst. Growth* **181**, 160 (1997).
5. A. C. Chiang, Y. Y. Lin, T. D. Wang, Y. C. Huang, and J. T. Shy, *Opt. Lett.* **27**, 1815 (2002).
6. B. Sturman, M. Aguilar, F. Agulló-López, V. Pruneri, and P. G. Kazansky, *J. Opt. Soc. Am. B* **14**, 2641 (1997).
7. E. Podivilov, B. Sturman, M. Goul'kov, S. Odoulov, G. Calvo, F. Agulló-López, and M. Carrascosa, *J. Opt. Soc. Am. B* **19**, 1582 (2002).
8. K. Peithmann, J. Hukriede, K. Buse, and E. Krätzig, *Phys. Rev. B* **61**, 4615 (2000).
9. S. Miyazawa, *J. Appl. Phys.* **50**, 4599 (1979).
10. L. E. Myers, R. C. Eckardt, M. M. Fejer, R. L. Byer, W. R. Bosenberg, and J. W. Pierce, *J. Opt. Soc. Am. B* **12**, 2102 (1995).
11. U. Schlarb and K. Betzler, *Phys. Rev. B* **48**, 15613 (1993).
12. R. S. Weis and T. K. Gaylord, *Appl. Phys. A* **37**, 191 (1985).
13. H. Kogelnik, *Bell Syst. Tech. J.* **48**, 2909 (1969).
14. K. Nassau, H. J. Levinstein, and G. M. Loiacono, *Appl. Phys. Lett.* **6**, 228 (1965).
15. U. Hartwig, K. Peithmann, B. Sturman, and K. Buse, *Appl. Phys. B* **80**, 227 (2005).
16. S. Kurimura and Y. Uesu, *J. Appl. Phys.* **81**, 369 (1997).
17. F. Kahmann, R. Matull, R. A. Rupp, and J. Seglins, *Phase Transitions* **40**, 171 (1992).
18. V. Grubsky, S. MacCormack, and J. Feinberg, *Opt. Lett.* **21**, 6 (1996).
19. R. Jungen, G. Angelow, F. Laeri, and C. Grabmaier, *Appl. Phys. A* **55**, 101 (1992).
20. F. Laeri, R. Jungen, G. Angelow, U. Vietze, T. Engel, M. Würtz, and D. Hilgenberg, *Appl. Phys. B* **61**, 351 (1995).
21. H. T. Hsieh, D. Psaltis, O. Beyer, D. Maxein, C. van Korff Schmising, K. Buse, and B. Sturman, *Opt. Lett.* **30**, 2233 (2005).